

Metapopulation dynamics in a complex ecological landscape

E. H. Colombo^{1,*} and C. Anteneodo^{1,2,†}

¹*Department of Physics, PUC-Rio, Rio de Janeiro, Brazil*

²*Institute of Science and Technology for Complex Systems, Rio de Janeiro, Brazil*

We propose a general model to study the interplay between spatial dispersal and environment spatiotemporal fluctuations in metapopulation dynamics. An ecological landscape of favorable patches is generated like a *Lévy dust*, which allows to build a range of patterns, from dispersed to clustered ones. Locally, the dynamics is driven by a canonical model for the evolution of the population density, consisting of a logistic expression plus multiplicative noises. Spatial coupling is introduced by means of two spreading mechanisms: diffusive dispersion and selective migration driven by patch suitability. We focus on the long-time population size as a function of habitat configurations, environment fluctuations and coupling schemes. We obtain the conditions, that the spatial distribution of favorable patches and the coupling mechanisms must fulfill, to grant population survival. The fundamental phenomenon that we observe is the positive feedback between environment fluctuations and spatial spread preventing extinction.

PACS numbers: 87.23.Cc, 89.75.Fb, 05.40.-a

I. INTRODUCTION

Habitat fragmentation is commonly observed in nature associated with heterogeneity in the distribution of resources, e.g., water, food, shelter sites, physical factors such as light, temperature, moisture, and any feature able to affect the growth rate of the population of a given species [1]. A fragmented population made of subpopulations receives in the literature the suitable name of *metapopulation* [1–3]. These fragments, also known as patches, are not completely isolated as they are coupled due to movements of individuals in space. For modeling purposes, as a first step one can adopt a single patch viewpoint, taking into account the impact of the surrounding population in an effective manner [4–7]. As a further step beyond the single patch level, one can resort to a spatially explicit model. From this perspective, deterministic and stochastic theoretical models have been developed to obtain the macroscopic behavior of the whole population [2, 8–12]. One of the main results is the detection of critical thresholds that delimit the conditions for the sustainability of the population, which occurs for a suitable combination of diverse factors, related to quality and spatial structure of the habitat, migration strategies and extinction rates. Here, we address related fundamental questions in metapopulation theory proposing a model that includes a general dispersion process, incorporating random and selective dispersal strategies. Additionally, we investigate the model dynamics on top of a complex ecological landscape whose spatial structure can be tuned, ranging from spread to aggregated patches.

Let us start from the local dynamics perspective. Locally, each patch has its dynamics driven primarily by reproduction and intraspecific competition (carrying ca-

capacity). Therefore, we assume that the deterministic factors that rule the evolution of the local population can be modeled by the logistic or Verhulst expression [13]. Stochasticity is introduced in real systems by the inherent complexity of the fluctuating environment (external noise) or by the variations in the birth-death process (internal, demographic noise) [2, 7, 14, 15], hence it has to be also taken into account. These deterministic and stochastic rules, along the lines of the canonical modeling [4, 14, 15], constitute the local component of our model. We assume that this local dynamics takes place on each site of a lattice, where we construct a complex arrangement of favorable and unfavorable patches. We define as favorable patches those sites that induce positive growth at low densities and as unfavorable patches those that are adverse to support life. A typical configuration of the model system in a square lattice is illustrated in Fig. 1.

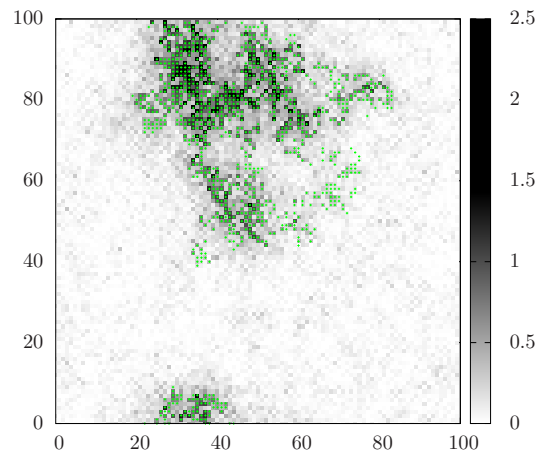


Figure 1. Ecological landscape (a green cross denotes the presence of a favorable patch) and population density distribution (in gray scale).

* eduardo.colombo@fis.puc-rio.br

† celia.fis@puc-rio.br

Spatial coupling is introduced by migrations from one patch to another. First, let us assume that spatial spread is conservative, preserving the number of individuals during travels and also that it is nonlocal, in the sense that individuals can travel long distances over the landscape, for example like butterflies and birds [8, 16]. We model the populational exchange between patches based on two behavioral strategies: one where the individuals spread in space diffusively, driven by density differences, and another where individuals transit selectively, mainly driven by patch-quality differences. These strategies can be linked to the amount of spatial information acquired by the individuals [17]. If they do not have any information about the spatial distribution of favorable patches, random movements emerge. In fact, this has been the focus of works on animal foraging, where optimal efficiency in resource search occurs without previous knowledge of food distribution [18]. This type of behavior has isotropy as a main trait, indicating directional indifference. Instead, if individuals have information on the distribution of favorable patches, some directions will be preferred.

In Sec. II, we will describe in detail each part of the model. The spreading process and spatial configuration of the ecological landscape are described in Secs. II A and II B, respectively. The results, reported in Secs. III and IV, focus on the impact of the spatial arrangement of the habitat on its overall viability, that is, on the long-time behavior of the population size. Mainly numerically, and with the aid of analytical considerations, we investigate the impact of habitat topology, spread range and stochasticity in the long time behavior of the population size, compared to the corresponding uncoupled metapopulation.

II. MODEL

In mathematical terms, we assume that the evolution of the population density (number of individuals per unit area), u_i , in each patch i is described by

$$\dot{u}_i = a_i u_i - b u_i^2 + D \Gamma_i[u] + \sigma_\eta u_i \bullet \eta_i(t) + \sigma_\xi \sqrt{u_i} \circ \xi_i(t), \quad (2.1)$$

where the constants a_i , b , D are the growth rate, the intraspecific competition coefficient and the spatial coupling coefficient. The noises η_i and ξ_i introduce environment and demographic stochasticities, respectively. They are assumed to be mutually independent zero mean and unit variance Gaussian white noises. The intensities of these multiplicative noises are controlled by coefficients σ_η and σ_ξ . The environmental noise term is expected to have external origins, then, its correlation even if small is non-null, justifying the use of Stratonovich calculus (\bullet); at the same time, the demographic noise represents fluctuations in the reproduction process of each independent individual, then Itô calculus is more suitable (\circ) [4, 14, 19]. These contributions define a local dynamics, at each site, ruled by Eq. (2.1) with $D = 0$, which is

known as canonical model [4]. We incorporate the additional term $D\Gamma_i[u]$ into Eq. (2.1) to account for the non-local contribution arising from fluxes between patches, as it will be explained below. This is the term that couples the set of stochastic differential equations (2.1).

The intrinsic growth rate of each patch i is quantified by the growth rate a_i , that can take positive or negative values. Patches can be favorable (or not), promoting growth (or decrease) of the local population, with $a_i = A_i^+ > 0$ (or $a_i = A_i^- < 0$). For the sake of simplicity, we consider a binary landscape, where sites can be in any of two states, $A_i^+ = -A_i^- = A > 0$, as assumed in previous studies [20, 21].

A. Nonlocal coupling

In order to define the coupling scheme let us state some considerations. First, note that it is reasonable to assume that active individuals like butterflies, birds, terrestrial animals use their perception and memory to increase the efficiency in the search for viable habitats. The spatial information stored by the individuals can yield optimized routes between favorable regions. In fact, there is a relation between spatial memory and migration strategy [17]. We introduce this trait by allowing individuals to have access to information about the spatial distribution of patch quality. Spatial knowledge can be acquired, for instance, by a direct verification in a previous visit or by the perception of the collective dynamics. Otherwise, if individuals do not have any information about the ecological landscape, or if they do not have memory, uncorrelated trajectories can emerge.

We contemplate both scenarios by modeling spread through a diffusive component together with a contribution of direct routes connecting favorable patches, governed by quality differences. The relative contribution of both mechanisms is regulated by parameter δ , with $0 \leq \delta \leq 1$ tuning from the ecologically driven ($\delta = 0$) to the purely diffusive ($\delta = 1$) cases. Moreover, we assume that coupling is weighted by a factor $\gamma(d_{ij})$ that decays with the distance d_{ij} between patches i and j , as will be defined below. Then, the flux J_{ij} from patch i to j is given by

$$J_{ij} = [\delta + (1 - \delta)\alpha_{ij}] \gamma(d_{ij}) u_i \geq 0, \quad (2.2)$$

where $\alpha_{ij} \equiv (a_j - a_i)/(4A) + 1/2$. Hence, the total flux is

$$\begin{aligned} \Gamma_i[u] &= \sum_{j \neq i} (J_{ji} - J_{ij}) \\ &= \sum_j \gamma(d_{ij}) [\delta(u_j - u_i) + (1 - \delta)(\alpha_{ji} u_j - \alpha_{ij} u_i)]. \end{aligned} \quad (2.3)$$

The total density is conserved by the exchanges described by Eq. (2.3), as can be seen by summing over i . It indicates that individuals tend to move towards patches with

fewer individuals and better quality. For $\delta = 1$, Eq. (2.3) represents a generalization of the Fick's law for nonlocal dispersal driven by density gradients. For $\delta = 0$, with our definition of α_{ij} , and binary patch growth rate, the possible values of $\alpha_{ji}u_j - \alpha_{ij}u_i$ are

$j \backslash i$	A	$-A$
A	$(u_j - u_i)/2$	u_j
$-A$	$-u_i$	$(u_j - u_i)/2$

This means that, when the quality of two patches is different, the flux occurs in the direction of the higher quality, weighted by the out-flowing population density (lowest quality patch). Only when the quality is the same, diffusive exchange can occur, to allow a network of favorable patches.

Concerning the factor that takes into account the distance between patches, there is empirical evidence [8, 22] that the frequency of occurrence of flights between patches decays with the distance, which is reasonable due to the increase of energetic cost. Although diverse decay laws are possible, we will assume exponential decay of the weight γ with the traveled distance ℓ , as observed for some kinds of butterflies [8, 22, 23], that is

$$\gamma(\ell) = \mathcal{N}^{-1} \exp(-\ell/\ell_c), \quad (2.4)$$

where ℓ_c is a characteristic length (the average traveled distance) and the normalization constant \mathcal{N} is such that the sum of the contributions of all patches equals one. Operationally, we will truncate the exponential at $\ell \simeq 8\ell_c \ll L$, where L is the linear characteristic size of the landscape.

B. Ecological landscape

In nature, the arrangement of the ecological landscape is built by many distinct processes, occurring in many time scales, creating complex spatiotemporal structures. Then, beyond the inclusion of the environmental noise η , it is also important to take into account the spatial organization of patches [8, 9, 24, 25].

Heterogeneity and patchiness are adequate to capture the complexity of diverse ecological systems [26–30]. Here we propose to use as complex ecological landscape a *Lévy dust* [18] distribution of favorable patches on a square domain of size $L \times L$ patches, with periodic boundary conditions. Over a background of adverse patches ($a_i = -A$), we construct a Lévy dust of favorable patches ($a_i = A$) given by the sites visited by a Lévy random walk with step lengths ℓ drawn from the probability density function $p(\ell) \propto 1/\ell^\mu$, with $1 \leq \ell \leq L$. This protocol has been used in the study of different problems [18, 27, 28], but we apply it here in the study of metapopulation dynamics. It allows to mimic a general class of realistic conditions [26, 28–30] and to tune different habitat landscapes through parameter μ , from

widely spread (for $\mu = 0$) to compactly aggregated in a few clusters separated by large empty spaces (for $\mu = 3$), as illustrated in Fig. 2.

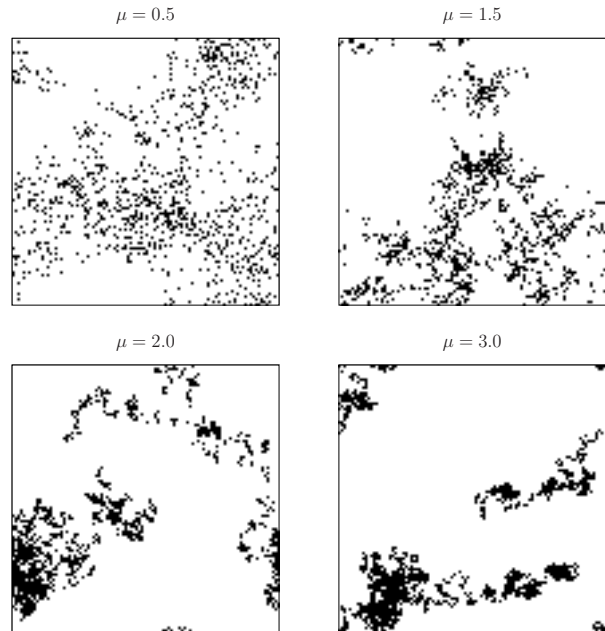


Figure 2. Habitat topology for different values of the exponent μ . Black cells indicate positive growth rate A and white cells negative growth $-A$, in a square domain of linear size $L = 100$. The density of favorable patches is $\rho = 0.1$.

We quantify the change in the spatial structure by computing the probability distribution of the *minimal*

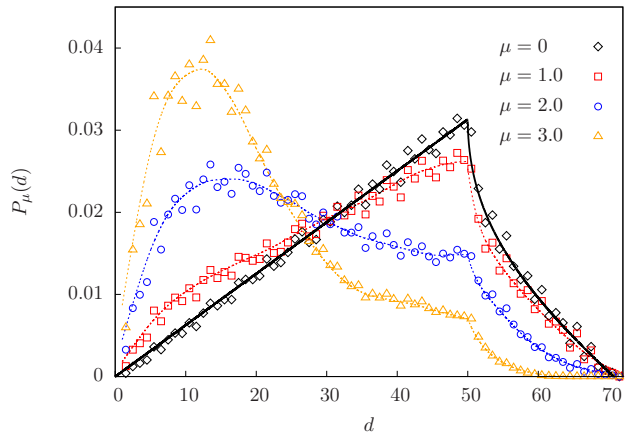


Figure 3. Probability distribution of the *minimal* distance between favorable patches for different values of μ , for $\rho = 0.1$ and $L = 100$ (100 configuration were used). Fluctuations are due to the discrete nature of the possible distances in the lattice. The dotted lines are a guide to the eye. The solid line represents the probability distribution for the distance between uniformly distributed random points in continuous space, drawn for comparison.

distance d between favorable patches $P_\mu(d)$ (see Fig. 3). For the density $\rho = 0.1$ used in the figure, when $\mu \lesssim 1$, patches are typically far from each other. For high values ($\mu \gtrsim 3$), the generating walk approaches the standard random walk, creating a much more clustered structure, evidenced by the peak at short distances. However the shape of $P_\mu(d)$ changes with ρ . When the patch density ρ is high, the shape of $P_\mu(d)$ resembles that of the uniform arrangement even for large μ , while at low densities $P_\mu(d)$ presents a peak at small d since the resulting configuration of patches is very localized even for small μ , as will be discussed in Sec. IV C. Furthermore, $P_\mu(d)$ is also sensitive to L , but we kept L fixed ($L = 100$), even if some properties may have not attained the large size limit, as far as μ and ρ allow to scan many qualitatively different possibilities of landscape structure.

Concerning the factor γ_μ that reflects the topology, as defined in Eq. (A3), it is affected by ρ more through the amount of favorable patches n_v than by its indirect consequences on the spatial distribution P_μ .

C. General considerations about the model

The set of parameters $\{D, \delta, \ell_c\}$ regulate the nonlocal dynamics. While D is the strength of the nonlocal coupling, δ controls the balance between diffusion and directed migration, and ℓ_c defines the coupling range. The ecological landscape is characterized by μ and ρ .

In the results presented in the following sections, we will restrict the analysis to a region of parameter space relevant to discuss the main phenomenology of the model. Thus, we will set $A = b = 1$ in all cases. We will also consider $L = 100$ and typically $\rho = 0.1$. Concerning the noise parameters, we set $\sigma_\eta = \sigma_\xi = 0$ to analyze the deterministic case in Sec. III and turn noise on by setting $\sigma_\eta = \sigma_\xi = 1$ in Sec. IV. This choice is based on previous works [4, 14]. Indeed, population size can be subject to large fluctuations as demonstrated by experimental data [16].

We performed numerical simulations of Eq. (2.1) on top of different landscapes, by preparing the system in the stationary state of the deterministic and uncoupled case, i.e., $u_i(0) = \max\{a_i/b, 0\}$ for all i , plus a small noise. Integration of Eq. (2.1) was carried out with Euler-Maruyama scheme with a time step $\Delta t = 10^{-3}$.

III. DETERMINISTIC CASE ($\sigma_\eta = \sigma_\xi = 0$)

Before proceeding to study the full model, we consider the deterministic case. Locally, when stochastic contributions are neglected, the asymptotic value of the population size for each patch is $u_i = a_i/b$. Introducing non-local effects, the population size might change. If population exchanges between patches are guided solely by their quality ($\delta = 0$), then, the favorable-patch network

will conserve the initial population size, so no interesting phenomena occur from the viewpoint of extinction. However, when $\delta > 0$, the diffusive behavior induces exploration of the neighborhood independently of habitat quality, which leads to the occupation of unfavorable regions making likely the death of individuals.

By numerical integration of Eq. (2.1) we obtain the time evolution of the total population density $n(t) = \sum_{i=1}^{L^2} u_i(t)$. In Fig. 4 we show the outcomes for fixed values of the model parameters and different initial conditions (different landscapes). While some of the realizations lead to exponential decay of the population other ones attain finite values at long times. Several different non null steady states can be attained. Notice however, that the steady values of different realizations are all below that of the uncoupled case, $\rho L^2 A/b = 1000$ for the parameters of the figure. Hence, diffusion favors the decrease of the total population density and the occurrence of extinctions, as expected.

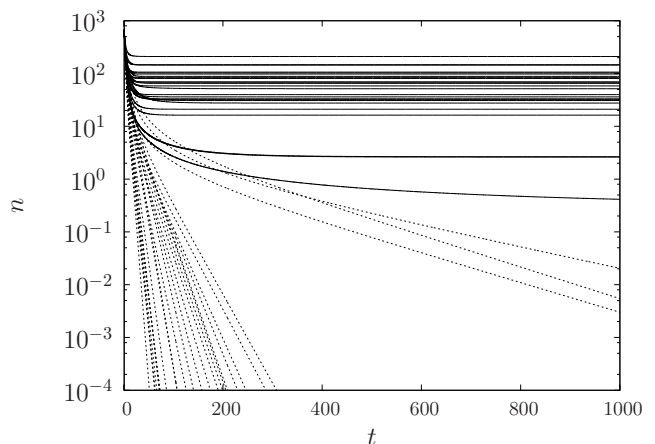


Figure 4. Deterministic ($\sigma_\eta = \sigma_\xi = 0$) time evolution of the total population density n , for $\delta = 1$, $\rho = 0.1$, $D = 10$, $\ell_c = 0.5$, $\mu = 1.7$, and different initial landscapes. This set of values results in about half of 50 realizations leading to extinction. We use a dotted line to flag the ones that tend to extinction exponentially fast and a solid line for those that lead to population survival.

In order to investigate how the fraction of survivals changes with the topology, we plot in Fig. 5 the number of survivals per realization, f_s , as function of μ , for several values of D . Besides the initial condition used throughout this paper (see Sec. II C), we observed that a perturbation of the null state also leads to the same results of Fig. 5. For given μ , increasing D favors the occurrence of extinctions as already commented above. For given D , below a threshold value of μ the population gets extinguished in all the realizations, while above a second threshold it always survives (for the finite number of realizations done), between thresholds both states, the null and non null ones, are accessible. The number of non null stable states increases with μ .

Summing over all i the deterministic form of Eq. (2.1), one finds that the steady solution $\dot{n} = 0$ must satisfy $\sum_i A_i u_i = b \sum u_i^2$, which has infinite solutions between the fundamental null state and the uncoupled case solution (the only stable one for $D = 0$). The condition for stationarity of the total density depends only on the local parameters, since fluxes are only internal, however, the coupling and landscape can stabilize configurations other than the trivial ones. Furthermore, in the Appendix, we performed an approximate calculation to show that, for small D , the null state is stable if

$$A - D(1 - \gamma_\mu) > 0, \quad (3.1)$$

where $0 \leq \gamma_\mu \leq 1$ is a factor that mirrors the topology, varying from $\gamma_\mu = \rho$ for the uniform case $\mu = 0$ to $\gamma_\mu = 1$ in the limits of large μ or large ρ . Despite this approximate expression fails in providing accurate threshold values, it predicts that survival is facilitated by larger A and spoiled by increasing D . It also qualitatively predicts the impact of the topology, as far as it indicates that the destructive role of diffusion can be compensated by a large enough degree of clusterization of the resources given by large γ_μ .

IV. STOCHASTIC CASE

First let us review some known results about the local (one site) dynamics, which is obtained in the limit $D \rightarrow 0$ of Eq. 2.1 (canonical model). In the deterministic case, the two-state habitat [20, 21] leads to local extinction (if $a_i = -A$) or finite population (if $a_i = +A$). The presence of stochastic contributions changes the stability of the patches. When $a_i = -A < 0$, the local extinction event predicted deterministically is reinforced by noise.

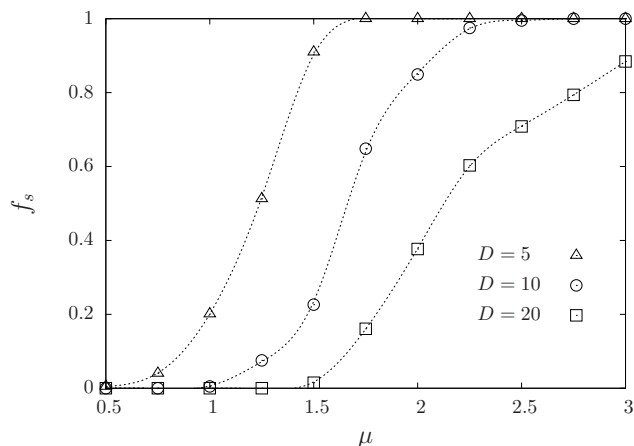


Figure 5. Fraction of surviving metapopulations f_s (over 100 realizations) in the deterministic case ($\sigma_\eta = \sigma_\xi = 0$) as a function of μ , setting $\delta = 1$, $\rho = 0.1$, $\ell_c = 0.5$, for the values of D indicated on the figure. In this and following figures, dotted lines are a guide to the eye.

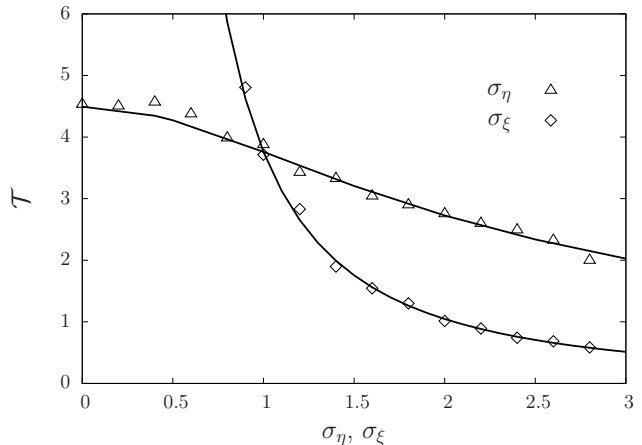


Figure 6. Single patch dynamics. Mean extinction T time vs σ_ξ (for $\sigma_\eta = 1$) and vs σ_η (for $\sigma_\xi = 1$). Symbols correspond to numerical simulations averaged over 500 samples and the full lines to the theoretical prediction given by Eq. (4.1). The curve for variable σ_ξ diverges in the limit $\sigma_\xi \rightarrow 0$.

For $a_i = +A > 0$, the demographic noise ξ , leads to extinction in a finite time that diverges as $\sigma_\xi \rightarrow 0$ [4, 6]. The external noise η reduces the most probable value of the population size, that becomes very close to zero when $\sigma_\eta > \sqrt{2A/b}$ [31].

The population stability can be quantified by the mean time to extinction \mathcal{T} averaged over realizations starting at $u(0)$. For Eq. (2.1) with $D = 0$, \mathcal{T} is given by [14],

$$\mathcal{T} = \int_0^{u_0} \int_z^\infty \frac{\exp(\int_z^v \Psi(u) du)}{V(v)} dv dz, \quad (4.1)$$

where $\Psi(u) = 2M(u)/V(u)$, with $M(u) = au - bu^2 + \sigma_\eta^2 u/2$ and $V(u) = \sigma_\eta^2 u^2 + \sigma_\xi^2 u$. The results of Eq. (4.1) are in good accord with those from numerical simulations, as illustrated in Fig. 6. When the noise intensity decreases, the time to extinction always increases, being divergent in the limit $\sigma_\xi \rightarrow 0$.

A. From local to global behavior

In this section we investigate the effects introduced by patch coupling, i.e., when $D \neq 0$. Nonlocal contributions redistribute the individuals in space, driven by density and quality gradients. In Fig. 7 we show that $D \neq 0$ prevents the extinction events that occur when $D = 0$ (see Fig. 6). Therefore, in contrast to the deterministic case, now spatial coupling is constructive. On the other hand, noise has also a constructive role when $D \neq 0$, differently to the uncoupled case, not only preventing extinction but also contributing to the increase of the population (as in the case $D = 10$). In a previous work [7], we already observed the constructive role in population growth of linearly multiplicative Stratonovich noise in contrast with

the destructive behavior of its Itô version. Therefore, environmental noise and coupling have a positive feedback effect on population growth, as shown in Fig. 7.

We will compute the long-time total population density $n_\infty \equiv \lim_{t \rightarrow \infty} n(t)$, which is useful to be compared with the initial value $n_0 \equiv n(0) = \rho L^2 u_0 = \rho L^2 (A/b)$, that represents the asymptotic total density in the deterministic uncoupled case. Then we will measure the ratio $E \equiv \langle n_\infty \rangle / n_0$, that represents a kind of efficiency, where the brackets indicate average over landscapes and noise realizations.

In the upper panel of Fig. 8 we plot the ratio E as a function of D . We see that for very small values of D , the population is non null, although the ratio E is smaller than one. Moreover, for given D , the ratio E is smaller when the diffusive component is absent ($\delta = 0$). In all cases the ratio first increases with D and even exceeds the value $E = 1$, indicating again that not only the noise has a constructive role in preventing extinction but also in promoting the increase of the initial total population. When diffusion is present ($\delta > 0$), the increase of E occurs up to an optimal value of the coupling D (with $E > 1$), above which the ratio decays. Hence, there is a nonlinear effect that does not reflect the linear combination in Eq. (2.2), as shown in the lower panel of Fig. 8. The diffusive component, despite being much less efficient, like in placing individuals in unfavorable regions, acts with greater connectivity. Then, for small D , the nonlocal contribution of the diffusive coupling is much higher than in the $\delta = 0$ case, leading to a higher population size. In fact, the abrupt transition in the connectivity of the spatial coupling is mirrored in the abrupt change suffered by the ratio E as δ becomes non null. Contrarily, for high values of D , $\delta = 0$ is more efficient due to high damage caused by an intense dispersal to-

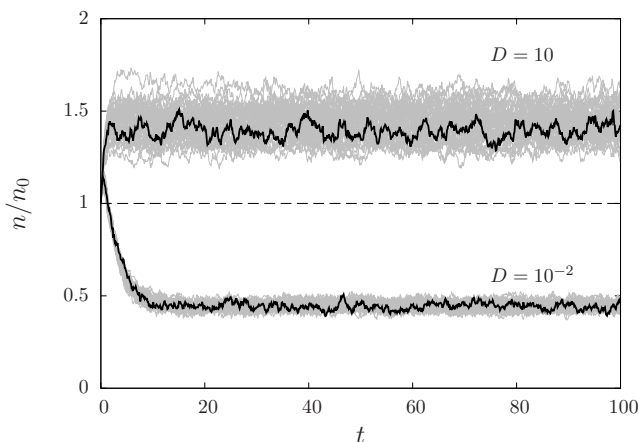


Figure 7. Temporal evolution of n/n_0 for $\delta = 0.5$, $\rho = 0.1$, $\ell_c = 0.5$, $\mu = 2.0$, $\sigma_\eta = \sigma_\xi = 1$ and values of D indicated on the figure. We highlight a single realization (black full line) for each set of 50 realizations (gray lines). The dashed line at $n = n_0$ is plotted for comparison.

wards unfavorable regions, which in the case of Fig. 8 are the majority of the sites. All these observations highlight the importance of the diffusive strategy, that can become more efficient than the ecological pressure driven by the quality gradient.

B. Habitat topology and coupling range

The nonlocal contribution results from the combination of the spread strategies, interaction range and topology, characterized by δ , ℓ_c and μ , respectively. Fig. 9 shows the ratio E as function of μ with different values of ℓ_c for $\delta = 1$ and $\delta = 0$.

$E > 1$ means that the combination of habitat topology and spatial coupling range leads the population to profit from the environment fluctuations, increasing its size. The region $E > 1$ is bigger when individuals are selective with respect to their destinations ($\delta = 0$) and

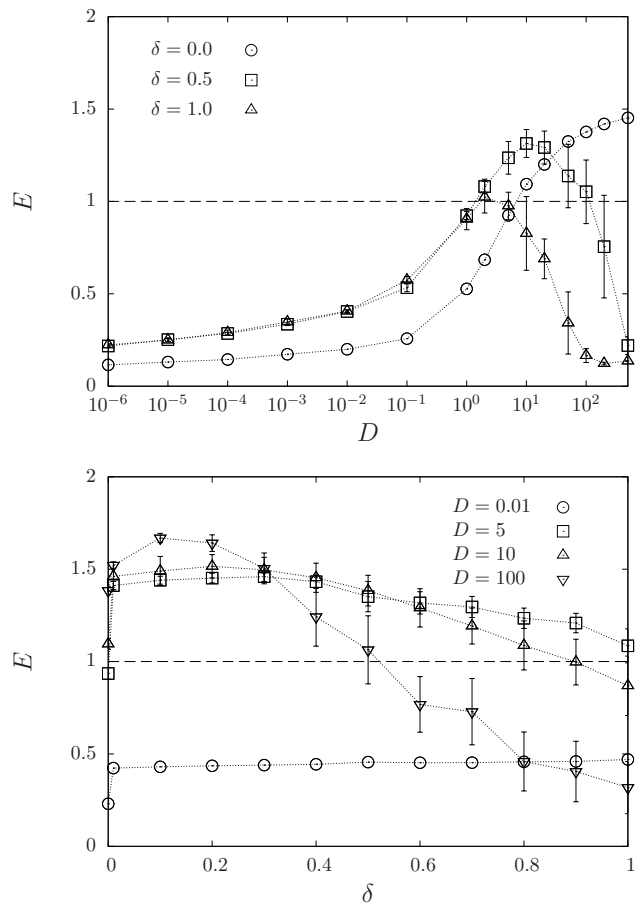


Figure 8. Ratio $E \equiv \langle n_\infty \rangle / n_0$ as a function of D (upper panel) for different values of δ , and E as a function of δ , for different values of D (lower panel), and $\rho = 0.1$, $\ell_c = 0.5$, $\mu = 2.0$ and $\sigma_\eta = \sigma_\xi = 1$. The symbols represent the average over 20 samples and the vertical bars the standard error. The dashed line at $E = 1$ is plotted for comparison.

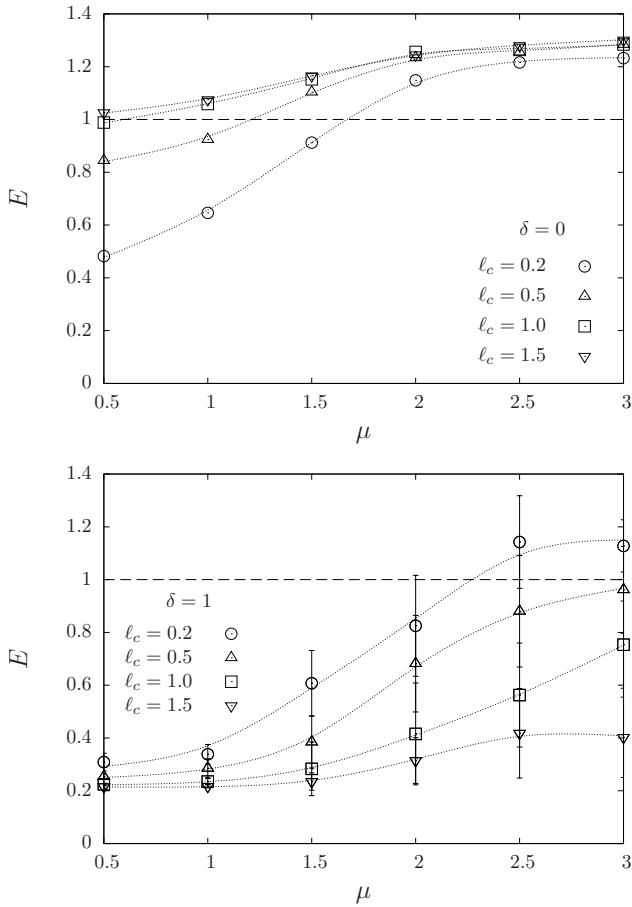


Figure 9. Ratio $E \equiv \langle n_\infty \rangle / n_0$, as a function of μ for different values of l_c , when $\delta = 0$ (upper panel) and $\delta = 1$ (lower panel), with $\rho = 0.1$, $D = 20$ and $\sigma_\eta = \sigma_\xi = 1$. The symbols represent the average over 20 samples and the vertical bars the standard error. The dashed line at $E = 1$ is plotted for comparison.

increases with l_c . For the diffusive strategy ($\delta = 1$), $E > 1$ is attained only in a clustered habitat (large μ) together with short-range dispersal (small l_c). We have already seen that in a sparse habitat, diffusion represents a waste, specially if the dispersal is long-range. Instead, when $\delta = 0$, the habitat does not need to be so clustered or the range so short for population growth. In this instance, the optimal combination occurs in a clustered habitat but with long-range coupling. Finally note that, as l_c increases, E becomes independent of the topology.

C. Density of favorable patches

Another important issue is the influence of the density ρ of favorable patches in the dynamics. Until now, we have kept it constant to highlight the effects of the heterogeneity of the habitat and of the coupling schemes in the longtime behavior of the total population size. In terms of the protocol used to generate the ecological landscape,

ρ not only changes the proportion of favorable patches but also reshapes the distribution of distances between favorable patches. In Fig. 10 we show three different outcomes of the spatial structure and the corresponding distance distribution for a fixed value of $\mu = 2$. For low ρ , patches organize in a kind of archipelago structure, that is much smaller than the system size, and the distance resembles that obtained for large μ when $\rho = 0.1$. For high ρ , many points of the domain are visited creating a distance distribution that approaches the homogeneous form. For μ higher than the value of the figure, profiles very similar to those shown in Fig. 10 are obtained. Meanwhile, for small values of μ , the distribution is almost invariant with ρ , being very close to that of the uniform case. This is due to frequent flights with lengths of the order of system size. Concerning the factor γ_μ that reflects the topology, as defined in Eq. (A3), it can be affected by ρ more through the amount of favorable patches n_v than by its indirect consequences on the spatial distribution P_μ .

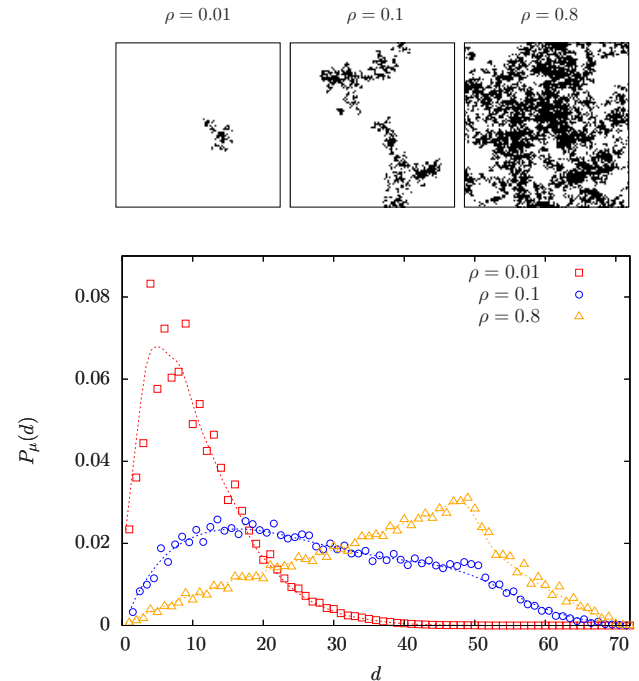


Figure 10. Spatial structure and probability distribution of the minimal distance between favorable patches (averaged over 100 landscapes), for $\mu = 2$ and three different values of ρ indicated on the figure.

In Fig. 11, we show the ratio E as a function of ρ for the case $\mu = 2$. By comparing the outcomes for different values of δ , we see the impact of distinct connectivities. In order to interpret this figure, recall that the initial population density n_0 is proportional to the number of favorable patches n_v , namely $n_0 = n_v A/b = \rho L^2$.

For $\delta = 1$, E presents a minimum value for $\rho \simeq 0.15$. Beyond this value, E grows with ρ attaining the value

of the full favorable lattice. In the opposite limit of vanishing ρ (no favorable patches), E diverges as far as, according to the model, (intrinsically) favorable patches are not necessary to promote growth due to the noisy growth rate. However, if noise is reduced, then the stochastic dynamics approaches the deterministic one, where the population will certainly go extinct.

Now, turning our attention to the $\delta = 0$ case, E is monotonically increasing with ρ , also attaining a limiting value when $\rho \rightarrow 1$. Differently from the diffusive case, there exists a critical value $\rho_c = 4 \times 10^{-4}$ ($n_v = 4$) for population survival.

For small ρ , it is curious that the role played by the connectivity, according to the model, makes the diffusive behavior more efficient, while selective moves are important at high values of ρ . In this case, when the system is approaching a fully favorable landscape, the ratio E tends to be the same for different values of δ . For intermediate values of ρ , we see that the selective strategy overcomes the diffusive one (but never overcomes the combined scheme).

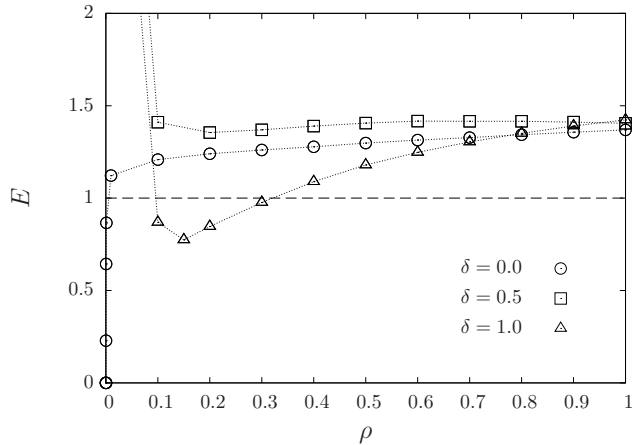


Figure 11. Ratio $E \equiv \langle n_\infty \rangle / n_0$ as a function of the favorable-patch density ρ , for $L = 100$. Different values of δ were also considered as indicated on the figure. The remaining parameters are $A = b = 1$, $D = 20$, $\ell_c = 0.5$, $\mu = 2.0$ and $\sigma_\eta = \sigma_\xi = 1$. The symbols represent the average over 20 samples and the vertical bars the standard error. The horizontal line represents $E = 1$.

V. CONCLUDING REMARKS

We implemented a general model in which the local dynamics, ruled by the canonical model [14], was coupled through different schemes on top of a complex landscape. This setting allowed to study the role of the habitat spatial structure and the stochastic fluctuations on the long-time state of the metapopulation. We restricted the analysis to a region of parameter space relevant to display the main features and the interplay between the different processes involved. For the deterministic case,

we have shown that, for small spread rates D , the distribution of favorable patches must be clustered enough for survival, while below a critical value of μ extinction occurs. For the stochastic case, we have shown that noise in combination with spatial coupling has a constructive role, that drives the population to survival, in contrast to the decoupled case where isolated patches would be extincted in finite time. We also studied the effects of the spreading strategy, pointing out that a mixed strategy (diffusive dispersion plus selective routes) will result in a larger population size (Fig. 8).

Furthermore, we analyzed the ratio E as a function of the coupling range ℓ_c and landscape parameter μ for different dispersal strategies. The more clustered, the more viable the environment is. For the selective strategy, the coupling range improves E , being more effective in disperse environments. The effect of the range saturates probably due to the rapid exponential decay of the weight function. In contrast, for the diffusive strategy, the coupling range plays an opposite role, as far as it drives individuals to unfavorable regions.

Our model could be improved in several directions. For instance by considering correlated environment fluctuations, exhaustible resources, etc. But, despite simple, the model shows the impact of spatial coupling, spatiotemporal fluctuations and their interplay, allowing to foresee the conditions for population survival as well as the optimal dispersal strategy.

Appendix A: Stability of deterministic steady states

In order to study how steady state stability is affected by spatial coupling, let us assume that the population is located at the favorable patches, which is true for small D (that is, close to the uncoupled case), and that the coupling is purely diffusive ($\delta = 1$). For a favorable patch, the deterministic form of Eq. (2.1) reads

$$\begin{aligned} \dot{u}_i &= Au_i - bu_i^2 + D \sum_{j \neq i} (u_j - u_i) \gamma(d_{ij}) \\ &= (A - D)u_i - bu_i^2 + D \sum_{j \neq i} u_j \gamma(d_{ij}), \end{aligned} \quad (\text{A1})$$

recalling that $\sum_{j \neq i} \gamma(d_{ij}) = 1$. To estimate the last term, that represents the flow of individuals from the neighborhood towards patch i , J_i^{in} , we consider that $u_j \approx u_i$. In this case

$$J_i^{in} = u_i \sum_{j \neq i} \gamma(d_{ij}), \quad (\text{A2})$$

where the sum effectively runs over the n_v favorable patches. The average over arrangements of a landscape $\gamma_\mu \equiv \langle \sum_{j \neq i} \gamma(d_{ij}) \rangle$ can be estimated as

$$\gamma_\mu = n_v \int P_\mu(\ell) e^{-\ell/\ell_c} d\ell. \quad (\text{A3})$$

It depends on μ and on the density ρ , such that it varies from ρ (when $\mu = 0$) to 1, in the extreme cases of either maximal density or very large μ . That is, γ_μ increases with μ , with ρ and with ℓ_c too. Then, Eq. (A1) can be approximated by

$$\dot{u}_i \simeq (A - D[1 - \gamma_\mu])u_i - bu_i^2 \equiv Gu_i - bu_i^2. \quad (\text{A4})$$

If $G > 0$, the population will grow and assume a finite value, bounded by the carrying capacity. Meanwhile, D diminishes the effective growth rate G , that becomes negative for sufficiently large D , namely for

$$D > A/(1 - \gamma_\mu) \quad (\text{A5})$$

indicating decrease of the population. In fact notice in Fig. 5 that the smaller D the less frequent the extinction events for a given μ . This effect can be mitigated by the landscape, through parameter γ_μ , when the density of favorable sites or clusterization associated with large μ increases. Eq. A5 also provides the linear stability condition for the null state. If $G < 0$, the population will decrease and go extincted.

ACKNOWLEDGEMENTS

C.A. acknowledges the financial support of Brazilian Research Agencies CNPq and FAPERJ. E.H.C. acknowledges financial support from Coordenação de Aperfeiçoamento de Pessoal de Nível Superior (CAPES).

-
- [1] I. Hanski and I. A. Hanski, *Metapopulation ecology*, Vol. 312 (Oxford University Press Oxford, 1999).
 - [2] I. Hanski, *Nature* **396**, 41 (1998).
 - [3] R. Levins, *Bulletin of the ESA* **15**, 237 (1969).
 - [4] O. Ovaskainen and B. Meerson, *Trends in Ecology & Evolution*, *Trends in Ecology & Evolution* **25**, 643.
 - [5] P. A. Hambäck and G. Englund, *Ecology Letters* **8**, 1057 (2005).
 - [6] B. Meerson and O. Ovaskainen, *Phys. Rev. E* **88**, 012124 (2013).
 - [7] L. A. da Silva, E. H. Colombo, and C. Anteneodo, *Phys. Rev. E* **90**, 012813 (2014).
 - [8] I. Hanski, M. Kuussaari, and M. Nieminen, *Ecology* **75**, pp. 747 (1994).
 - [9] I. Hanski and O. Ovaskainen, *Nature* **404**, 755 (2000).
 - [10] S. J. Cornell and O. Ovaskainen, *Theoretical Population Biology* **74**, 209 (2008).
 - [11] A. North and O. Ovaskainen, *Oikos* **116**, 1106 (2007).
 - [12] O. Ovaskainen, D. Finkelshtein, O. Kutoviy, S. Cornell, B. Bolker, and Y. Kondratiev, *Theoretical Ecology* **7**, 101 (2014).
 - [13] P. F. Verhulst, *Correspondance mathématique et physique* **10**, 113 (1838).
 - [14] H. Hakoyama and Y. Iwasa, *J. Theor. Biol.* **232**, 203 (2005).
 - [15] H. Hakoyama and Y. Iwasa, *J. Theor. Biol.* **204**, 337 (2000).
 - [16] T. H. Keitt and H. E. Stanley, *Nature* **393**, 257 (1998).
 - [17] J. M. Berbert and W. F. Fagan, *Ecological Complexity* **12**, 1 (2012).
 - [18] A. Ferreira, E. Raposo, G. Viswanathan, and M. da Luz, *Physica A* **391**, 3234 (2012).
 - [19] N. Kampen, *Journal of Statistical Physics* **24**, 175 (1981).
 - [20] C. R. Fonseca, R. M. Coutinho, F. Azevedo, J. M. Berbert, G. Corso, and R. A. Kraenkel, *PLoS ONE* **8**, e66806 (2013).
 - [21] R. Kraenkel and D. P. da Silva, *Physica A* **389**, 60 (2010).
 - [22] M. Baguette, *Ecography* **26**, 153 (2003).
 - [23] Z. Fric and M. Konvicka, *Basic and Applied Ecology* **8**, 377 (2007).
 - [24] L. J. Gilarranz and J. Bascompte, *J. Theor. Biol.* **297**, 11 (2012).
 - [25] J. Bascompte and R. V. Sole, *J Anim Ecol* **65**, 465 (1996).
 - [26] R. T. Forman, *Landscape Ecology* **10**, 133 (1995).
 - [27] O. Miramontes, D. Boyer, and F. Bartumeus, *PLoS ONE* **7**, e34317 (2012).
 - [28] N. Kenkel and D. Walker, *Abst. Bot* **17**, 53 (1993).
 - [29] G. Sugihara and R. M. May, *Trends in Ecology & Evolution* **5**, 79 (1990).
 - [30] A. Tsuda, *Journal of Oceanography* **51**, 261 (1995).
 - [31] W. Horsthemke and R. Lefever, *Noise-Induced Transitions: Theory and Applications in Physics, Chemistry, and Biology*, Springer complexity (Physica-Verlag, 2006).